

Article

Enhancement of the Activity of Electrochemical Oxidation of BPS by Nd-Doped PbO₂ Electrodes: Performance and Mechanism

Yan Zhang * , Zhili Ni and Jie Yao

Department of Civil Engineering, Zhejiang University, 866 Yuhangtang Road, Hangzhou 310058, China; nizhili@zju.edu.cn (Z.N.); 11812055@zju.edu.cn (J.Y.)

* Correspondence: zhangyan@zju.edu.cn; Tel.: +86-571-88206753; Fax: +86-571-88208721

Received: 10 March 2020; Accepted: 29 April 2020; Published: 7 May 2020



Abstract: The electrochemical oxidation processes have attracted tremendous attention on the destruction of toxic and non-biodegradable organics. A series of neodymium (Nd)-doped PbO₂ electrodes (Ti/PbO₂-Nd) were synthesized through a pulse electrodeposition method, and its activity of bisphenol S (BPS) removal was further examined. The morphologies and structures were characterized by the X-ray diffraction (XRD), scanning electron microscopy (SEM) and an energy dispersive spectrometer (EDS). The performance, energy consumption and mechanism of electrochemical oxidation of BPS by Ti/PbO₂-Nd electrode were also discussed. Compared to the traditional Ti/PbO₂ electrode, the Ti/PbO₂-Nd enables finer crystal particles, facilitating the oxygen evolution overpotential (OEP) from 1.41V to 1.55V and the generation of hydroxyl radicals (•OH). Moreover, lower duty cycles during the preparation of the electrode also contribute to the tapering size of crystals. The results show that the Ti/PbO₂-Nd electrode exhibits relatively high activity in the anodic oxidation of BPS. Over 95% of BPS could be removed with the current density of 15 mA cm⁻². Moreover, the energy consumption of BPS degradation on Ti/PbO₂-Nd electrode is 60.26 kWh m⁻³, much lower than that on Ti/PbO₂ electrode (95.45 kWh m⁻³). To conclude, the Ti/PbO₂-Nd electrode has been proven to be a promising material for BPS removal.

Keywords: bisphenol S; electrochemical degradation; Ti/PbO₂-Nd electrode; mechanism; duty cycle

1. Introduction

As a well-known endocrine disrupting chemical, the adverse impacts of bisphenol A (BPA) on human health have drawn much attention, and the use of BPA has even been prohibited in some countries [1,2]. As an alternative substitute of BPA, bisphenol S (BPS), which is considered to be more heat-stable and sunlight-resistant, has been adopted in various consumer products. However, increasing research has demonstrated that BPS may be leaked to the environment in the process of production, transportation and usage, and it has even been detected in water environments [3,4]. Importantly, BPS is found to be potentially harmful to humans as well as the ecosystem [5–7]. Moreover, BPS exerts remarkable effects on the structures and activities of trypsin and pepsin [8]. Therefore, it is of great importance and necessity to investigate the removal of BPS.

Degradation methods can be scarcely found to eliminate BPS from water. Shao et al. prepared ultrathin α -Fe₂O₃ nanosheets with a high percentage of exposed (110) facets, and found nearly 91% of BPS could be effectively degraded within 120 mins under visible lights [2]. However, low regeneration and unsuitability for the treatment of high-concentration organic wastewater made it limited for real application. Liu and his co-author revealed that a carbon-based iron catalyst (Fe@C) with peroxymonosulfate (PMS) activation could enhance the removal rate of BPS to 92.8% within 60

mins [9], but problems still exist in application [10]. Moreover, Danzl et al. found that only 24% of BPS could be adsorbed by activated carbon clothes (ACCs) with *E. coli* biodegradation [11].

Electrochemical degradation has been adopted as one of the most promising technologies in wastewater treatment. It is well known that the materials of electrodes determine the current efficiency and the removal efficiency of pollutants. Among the metal oxide electrodes, PbO₂ electrodes have shown good performances due to their high oxygen evolution overpotential (OEP), stability and low cost [12–15]. However, the active layer is easy to peel off during electrodegradation, leading to the decrease of the activity and stability of the electrode. Thus, the Sb-SnO₂ interlayer is added [16]. Meanwhile, corrosion of anodes during electrolysis also limits their service life [17]. Recently, the modifications of the traditional PbO₂ electrodes have been carried out to enhance the service life of the electrode and increase the active area of the electrode.

Therefore, a series of elements have been introduced into the PbO₂ electrodes, and rare earth metals have been regarded as the ideal ones [18–20]. The special 4f electronic structure of rare earth metals contributes to high efficiency in the catalytic oxidation of organics [21]. Xu et al. [22] prepared a Ce-doped Ti/nanoTiO₂/PbO₂ electrode and found that its large active surface area and small charge transfer resistance contributed to high electrocatalytic activity. Feng et al. [23] evaluated the performance of four typical anodes (i.e., Dy, Nd, Eu, Gd) for electrochemical degradation of phenol, and found that the Nd-doped anode exhibited the best electrocatalytic performance. Moreover, the Ni-Nd co-doped SnO₂-Sb anode was believed to be attributed to the improved generation of reactive oxygen species (ROS), which enhanced the degradation of phenol and the total organic carbon (TOC) [24]. Besides, the relaxation time during pulse electrodeposition for electrode preparation can enhance adsorption of inhibitory substances and then retard the growth of grains, so pulse electrodeposition may be an ideal method for the preparation of PbO₂ electrodes [25,26].

As BPS carries a phenol functional group, an electrochemical degradation method with rare earth-doped PbO₂ electrodes may be feasible for BPS removal. However, to the best of our knowledge, relevant research can be rarely found, and the same case goes to research on the preparation of Ti/PbO₂-Nd deposited in pulse electrodeposition methods. Thus, on the basis of the Ti/PbO₂ electrode, a series of Nd-doped Ti/PbO₂ electrodes (Ti/PbO₂-Nd) were prepared and used for the electrocatalytic removal of BPS.

The electrodes were fully characterized by scanning electron microscopy (SEM), an energy dispersive spectrometer (EDS) and X-ray diffraction (XRD). Their electrochemical properties were studied by linear sweep voltammetry (LSV) and cyclic voltammetry (CV). Moreover, the performance of Ti/PbO₂-Nd electrode for BPS removal, the influence of duty cycle during the preparation of the electrode and the doping amount of Nd in Ti/PbO₂-Nd electrode on BPS removal efficiency were evaluated. The energy consumption on Ti/PbO₂ and Ti/PbO₂-Nd electrodes were calculated. Besides, the reusability of Ti/PbO₂-Nd was also evaluated. The operating parameters on the electrocatalytic degradation of BPS, such as the current density and initial pH value, were also optimized. Finally, the mechanism of electrochemical oxidation of BPS by Ti/PbO₂-Nd was discussed. To sum up, the present research aims to find a promising electrode to further enhance the electrocatalytic activity of BPS.

2. Materials and Methods

2.1. Materials and Chemicals

A titanium plate (99.9%, 2 cm × 3 cm × 0.1 mm) was provided by Gaodewei Co., Ltd. (Beijing, China). The platinum sheet (99.99%) with the same area was provided by Saiaosi Co., Ltd. (Hangzhou, China). BPS, phosphoric acid (chromatographically pure) and acetonitrile (chromatographically pure) were obtained from Aladdin Medicine Co., Ltd. (Shanghai, China). Neodymium nitrate, SnCl₄·5H₂O and SbCl₃ were bought from Macklin Co., Ltd. All the other chemicals were purchased from Sinopharm Chemical Reagent Co., Ltd, and all solutions were prepared with deionized ultrapure water.

2.2. Electrodes Preparation

Before deposition, the titanium sheets were pre-treated through polishing followed by a 10-min ultrasonic cleaning in acetone, ethyl alcohol and deionized water, respectively. Then, the titanium sheets were etched in 40% NaOH solution at 80 °C for 2 h and then in 15% oxalic acid solution at 85 °C for another 2 h. Finally, they were rinsed with deionized ultrapure water. Then, the pretreated Ti sheets were brushed with the solution containing 2 g SbCl₃ and 20 g SnCl₄·5H₂O in 100 mL ethanol-HCl mixture at room temperature [27], followed by subsequent drying at 120 °C for 10 mins and then 500 °C for another 10 mins. The process was repeated 10 times before the final annealing at 500 °C for 70 mins.

Ti/PbO₂-Nd electrodes were prepared in the deposition solution composed of 0.3 mol L⁻¹ Pb(NO₃)₂, 0.02 mol L⁻¹ NaF and different concentrations of Nd(NO₃)₃ by pulse electrodeposition. F-doping is helpful for the deposition of the PbO₂ active layer on Ti substrate, and can reduce the internal stress between the coating and substrate and thus increase the service life of the electrode [28,29]. Hence, NaF was added in the deposition solution for preparing the Ti/PbO₂-Nd electrode. Meanwhile, the pH value was set as 2.0 by nitric acid. The pulse electrochemical deposition processes were performed in an undivided cylindrical vessel at 65 °C for 120 mins under the anodic current density of 5–20 mA cm⁻² and the duty cycles in 50%–100%. The prepared Ti sheets were set as the anode and Pt foil as the counter cathode.

The Ti/PbO₂ electrode was prepared under the same conditions without neodymium nitrate in 50% duty cycle, which was marked as 50%-Ti/PbO₂.

The duty cycle (γ) mentioned above is the percentage of total time in a pulse cycle given by:

$$\gamma = \frac{t_{on}}{t_{on} + t_{off}} \times 100\% \quad (1)$$

where t_{on} and t_{off} are the time of power on and power off, respectively. Ti/PbO₂-Nd electrodes are marked as γ -Ti/PbO₂-Nd, and when duty cycle is 100%, the electrode is also marked as DC-Ti/PbO₂-Nd.

2.3. Characterizations of Electrodes

The micro-morphologies of the Ti/PbO₂ electrode and Ti/PbO₂-Nd electrodes prepared in different pulse duty cycles were characterized by SEM (FEG650, FEI, USA). The contents of Nd in different Ti/PbO₂-Nd electrodes were measured by an energy dispersive X-Ray spectroscopy detector (EDS) fitted to the SEM. The crystal structures were identified by using XRD (XRD-7000, Shimadzu, Japan) with CuK α X-ray radiation source (40 kV, 30 mA). The 2 θ ranged from 20° to 80°.

The electrochemical properties tests were achieved by using an electrochemical workstation (CHI660e, Shanghai Chenhua, China). All tests were conducted in a typical three-electrode system at room temperature. The fabricated electrodes were used as anode, Pt sheet as counter electrode, and Ag/AgCl electrode as the reference electrode. In order to obtain the OEP of different electrodes, a linear sweep voltammetry (LSV) method was employed. The LSV tests were conducted in 0.2 mol L⁻¹ Na₂SO₄ solution with a scan rate of 1 mV s⁻¹. In addition, cyclic voltammetry (CV) curves were tested in a 0.2 mol L⁻¹ Na₂SO₄ solution with a scan rate of 10 mV s⁻¹.

2.4. Electrochemical Oxidation of BPS

The electrochemical oxidation of BPS was carried out by the CHI660e electrochemical workstation in a 250 mL single chamber glass reactor. The Ti/PbO₂ or Ti/PbO₂-Nd electrode and the equal-area Pt foil were set as the anode and cathode, respectively. Initial bath solutions were composed of 5 mg L⁻¹ BPS with 0.2 mol L⁻¹ Na₂SO₄ supporting electrolyte. Moreover, the electro-oxidation was performed under constant current density and a temperature of 15 mA cm⁻² and 25 °C, respectively. The pH was pre-adjusted by adding 0.1 mol L⁻¹ H₂SO₄ or 0.1 mol L⁻¹ NaOH. No buffer was added during the experiment.

Unless otherwise described, the experiments were carried out with temperature, pH and initial BPS concentration of 298 K, 5.5 and 5 mg/L, respectively.

2.5. Analytical Methods

Samples were periodically collected to analyze the concentration of BPS and to detect the intermediate products. The concentrations of BPS were analyzed by a high performance liquid chromatography coupled with UV detector (HPLC-UV, Agilent 1200), which was equipped with an XDB-C18 column (4.6×150 mm, 5-micron). The mobile phase, with a flow rate of 1.0 mL min^{-1} , was composed of acetonitrile and phosphoric acid solution (0.1%) in a ratio of 30:70 (*v/v*). The injected volume and the column temperature were set at 259 nm, 20 μL and 35°C , respectively. The intermediate products from the BPS degradation process were detected by an Agilent 1290 HPLC coupled with 6460 triple quadrupole mass spectrometry (HPLC-MS, USA). The positive mode electrospray ionization ((+) ESI) was used and the *m/z* range was set from 15 to 500. The fragmentor voltage was 135V. In addition, the mobile phase was composed of acetonitrile and formic acid solution (0.1%) in a ratio of 30:70 (*v/v*) with flow rate of 1.0 mL min^{-1} . Furthermore, the pH value was detected with a HACH LDO101 pH analyzer. The energy consumption (ξ) of BPS degradation on different electrodes is calculated as follows [21]:

$$\xi = \frac{P \times t}{V \times \lg(c_0/c_t)} \quad (2)$$

where ξ (kWh m^{-3}) is the energy consumption value, P (kW) is the output power, t (h) is the reaction time, V (m^3) is the bath solution volume, c_0 (mg/L) is the initial concentration of BPS, and c_t (mg/L) is the BPS concentration at time t .

3. Results and Discussion

3.1. Electrode Optimization

The influence of Nd in the Ti/PbO₂-Nd electrodes on the BPS removal was studied. The results are shown in Figure 1. Figure 1a shows that the BPS removal efficiency improves as the concentration of Nd increases. The highest BPS removal efficiency was 95.15% when the ratio of Pb:Nd was 10:1, which is 1.12 times higher than that of the Ti/PbO₂ electrode. Moreover, the electrocatalytic oxidization of BPS by Ti/PbO₂-Nd fits the pseudo first-order kinetics model, and the reaction rate constant reached $49.3 \times 10^{-3} \text{ min}^{-1}$ when the ratio of Pb:Nd was 10:1, which is much bigger than that of the Ti/PbO₂ electrode ($31.9 \times 10^{-3} \text{ min}^{-1}$). Therefore, the ratio of Pb:Nd = 10:1 in the Ti/PbO₂-Nd electrode is considered an ideal Nd-content, which was thus chosen in the following experiments unless otherwise specified.

The experiments of BPS removal by Ti/PbO₂-Nd electrodes prepared with different duty cycles were carried out. The results are shown in Figure 2. It can be seen that Ti/PbO₂-Nd electrodes prepared by pulse deposition performed better than that of those prepared in a continuous current. When the duty cycles of the Ti/PbO₂-Nd electrode prepared decreased from 100% (DC-Ti/PbO₂-Nd) to 50% (50%-Ti/PbO₂-Nd), the electrocatalytic removal efficiency of BPS increased from 66.79 to 95.15%. Moreover, the electrochemical oxidation of BPS fits the pseudo first-order kinetics well. Table 1 summarizes the kinetics coefficients (k) and correlation coefficients (R^2) of the BPS degradation process. The first-order kinetics constant decreased in the following order: 50%-Ti/PbO₂-Nd > 60%-Ti/PbO₂-Nd > 70%-Ti/PbO₂-Nd > 80%-Ti/PbO₂-Nd > DC-Ti/PbO₂-Nd. Therefore, unless otherwise specified, the 50%-Ti/PbO₂-Nd electrode was chosen for further study.

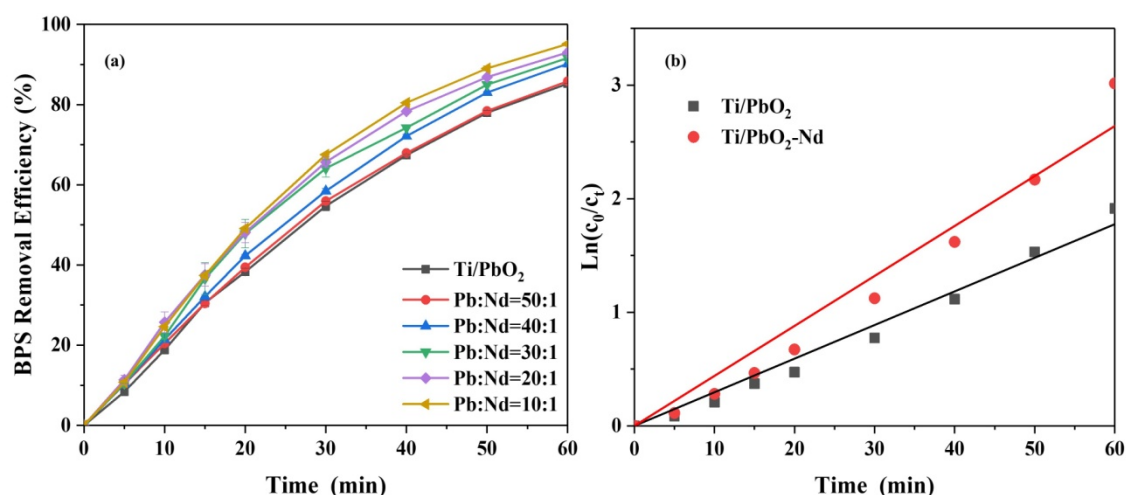


Figure 1. (a) Removal of bisphenol S (BPS) by Ti/PbO₂ or Ti/PbO₂-Nd electrodes with different Nd contents and (b) corresponding pseudo first-order kinetics (initial pH = 5.5; initial BPS concentration = 5 mg L⁻¹; T = 25 °C; Na₂SO₄ = 0.2mol/L; current density = 15 mA cm⁻²).

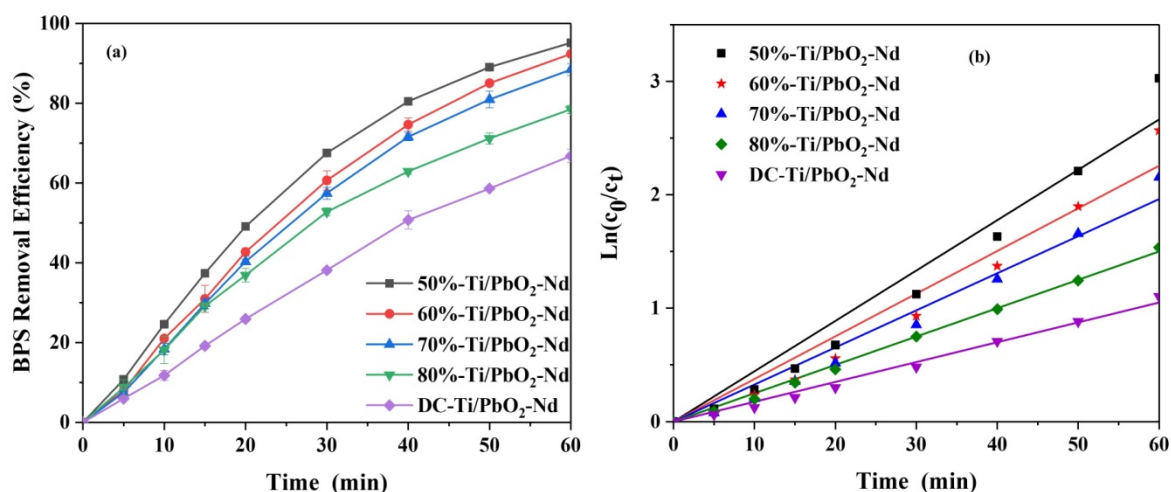


Figure 2. (a) Removal of BPS by Ti/PbO₂-Nd with different duty cycles and (b) corresponding pseudo first-order kinetics (initial pH = 5.5; initial BPS concentration = 5 mg L⁻¹; T = 25 °C; Na₂SO₄ = 0.2 mol/L; current density = 15 mA cm⁻²).

Table 1. Electrocatalytic activity of Ti/ PbO₂-Nd electrodes.

Duty Cycle	Kinetics Coefficientsk (10 ⁻³ min ⁻¹)	Correlation Coefficient R ²
50%	49.3	0.976
60%	42.2	0.974
70%	36.1	0.986
80%	25.8	0.999
100% (DC)	18.7	0.995

3.2. Morphology and Structure of Ti/PbO₂-Nd Electrodes

SEM images of Ti/PbO₂ and Ti/PbO₂-Nd electrodes are shown in Figure 3. It shows that the morphology of the Ti/PbO₂ electrode (Figure 3a) is composed of a mass of blocks in a typical coarse pyramidal shape. After doping Nd, the Ti/PbO₂-Nd electrode exhibited a finer crystal structure without sharp edges (Figure 3b). Studies show that the morphology structure of the electrode surface has a great impact on the nature of electrodes [30,31].

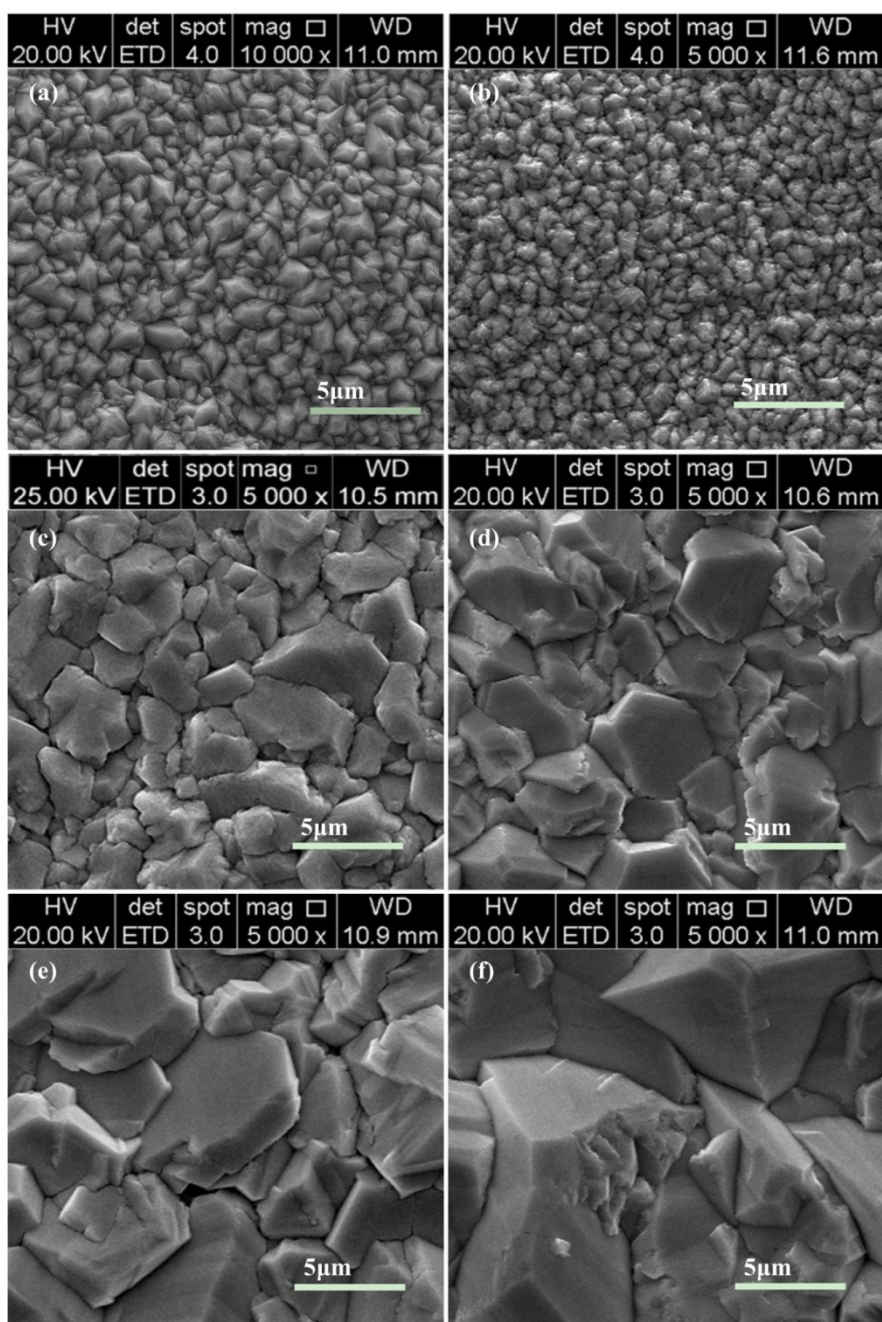


Figure 3. Images of (a) Ti/PbO₂ electrode deposited in 50% duty cycles and Ti/PbO₂-Nd electrodes deposited in duty cycles of: (b) 50%, (c) 60%, (d) 70% and (e) 80%, (f) 100%.

Figure 3b–e presents the surface morphologies of the Ti/PbO₂-Nd deposits fabricated in different duty cycles. The pulse current methods during the preparation will change the surface of Ti/PbO₂-Nd electrodes. Large dents can be found and the pyramid shape becomes inconspicuous. Moreover, the size of crystals got finer with a decrease in duty cycles. It is helpful to increase the specific surface area of the surface-active layer and enlarge the effective area of the electrode, thus leading to enhanced activity of the electrode which can explain the phenomenon in Figure 2.

The EDS spectrum of the Ti/PbO₂ and Ti/PbO₂-Nd electrodes are shown in Figure 4. It indicates that elements Pb and O exist in both Ti/PbO₂ and Ti/PbO₂-Nd electrodes. Moreover, element Nd was detected in Ti/PbO₂-Nd electrodes, demonstrating its successful doping. Meanwhile, the amount of

Nd in the electrode matrix was measured around 1.02 wt %. Furthermore, either Sn or Sb could be detected, indicating that the compact outermost layer completely covered the middle layer.

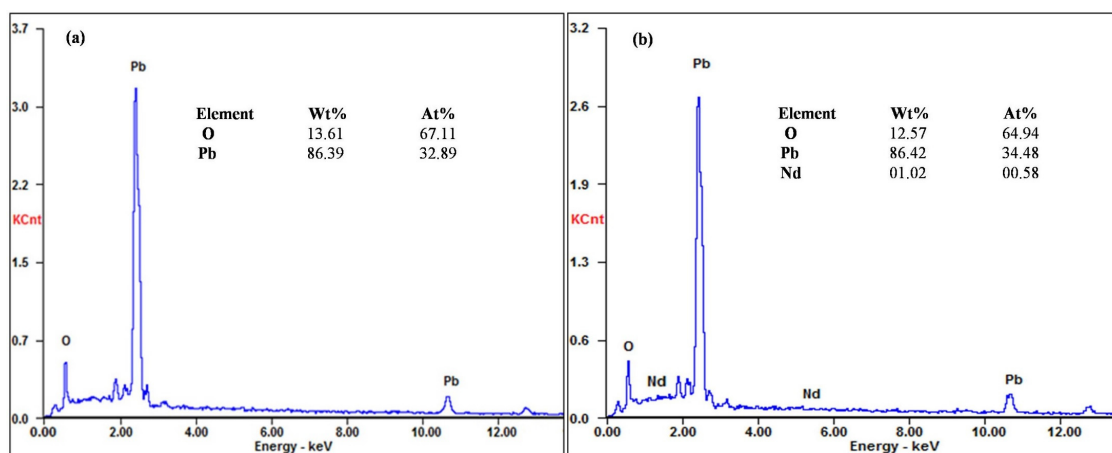


Figure 4. Energy dispersive X-Ray spectroscopy detector (EDS) spectra of (a) Ti/PbO₂ electrode and (b) Ti/PbO₂-Nd electrode.

Figure 5 shows different XRD patterns of Ti/PbO₂ and Ti/PbO₂-Nd electrodes. The β -PbO₂ phase can be found in both electrodes. According to the Joint Committee on Powder Diffraction Standards (JCPDS) card and previous research [32], diffraction peaks can be found at 25.4°, 32.0°, 49.0° and 62.3°, indicating the (110), (101), (211) and (301) plane of β -PbO₂ phase, respectively. Compared to Ti/PbO₂, a new bread-shaped diffraction peak at 29.9° was found on the Ti/PbO₂-Nd electrode, which is in great agreement with the neodymium oxide (Nd₂O₃) according to the standard card (JCPDS #83-1356). However, the XRD pattern of Nd was not obvious, suggesting a lower crystallinity of Nd than β -PbO₂ [22,30]. It can be attributed to a new-nucleate center of PbO₂ caused by Nd₂O₃, which prevents the further growth of PbO₂ grains [22]. When Nd was introduced, the (110) phase became the strongest peak rather than (301). Moreover, the intensity of (110) in Ti/PbO₂-Nd electrode was higher than (301) in the Ti/PbO₂ electrode, indicating that the preferred orientation of PbO₂ crystals is along the (110) direction [33]. Meanwhile, the characteristic peak of (301) in Ti/PbO₂ electrode was wider, showing an incomplete deposition [33]. In other words, Ti/PbO₂-Nd can be identified as an ideal electrode with good crystallinity.

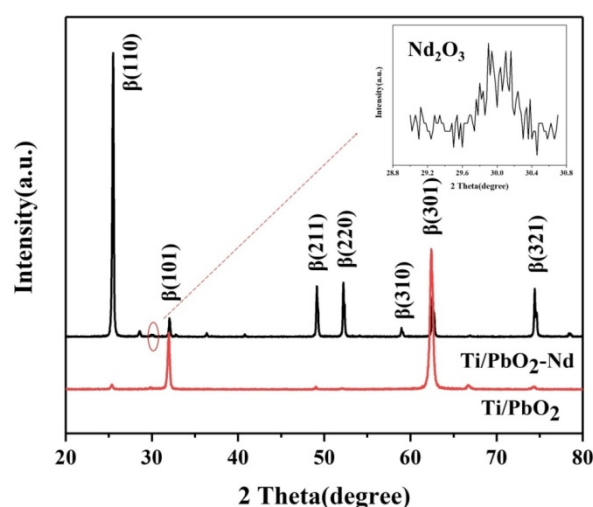


Figure 5. Spectra for Ti/PbO₂ and Ti/PbO₂-Nd electrodes.

3.3. Electrochemical Property of Ti/PbO₂-Nd Electrodes

Generally, oxygen evolution is an undesired reaction on the process of electro-oxidation. It is considered as a competitive reaction because of the consumption of reactive oxygen species. Figure 6 shows that the OEP of Ti/PbO₂ and Ti/PbO₂-Nd electrodes are 1.41 and 1.55 V vs. Ag/AgCl, respectively. After introducing the element Nd into PbO₂ electrode, the OEP increased. According to previous studies, a high OEP is beneficial to reduce the occurrence of oxygen evolution, indicating a higher utilization of hydroxyl radicals, high oxidation efficiency and low energy consumption [32]. In other words, high OEP leads to a high electrocatalytic activity of the electrode [34]. Thus, Ti/PbO₂-Nd electrodes have a better electrochemical property.

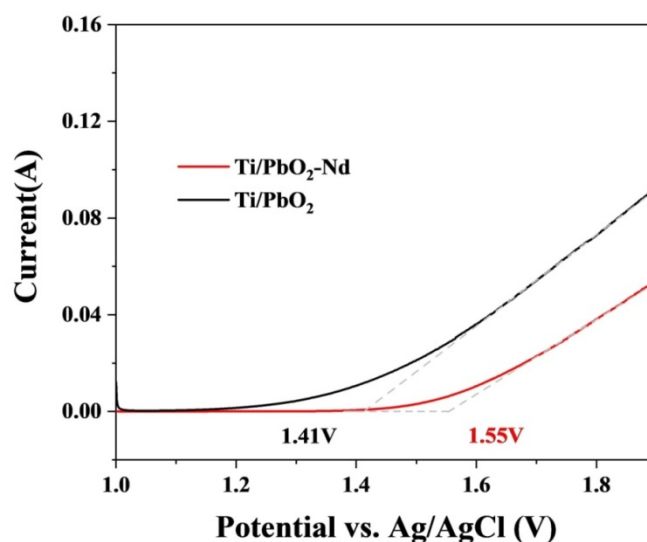


Figure 6. Linear sweep voltammetry (LSV) curves of Ti/PbO₂ and Ti/PbO₂-Nd electrodes.

Figure 7 presents the CV curves of Ti/PbO₂ and Ti/PbO₂-Nd electrodes. It should be noted that the oxidation peak detected on Ti/PbO₂-Nd electrode was higher than that on the Ti/PbO₂ electrode, indicating that the Ti/PbO₂-Nd electrode possesses a larger surface area. That is to say, Nd-doping helped a lot with increasing the specific surface area, which is consistent with SEM results (Figure 3). Thus, more •OH would be generated on the electrode surface which would enhance the electro-oxidation activity.

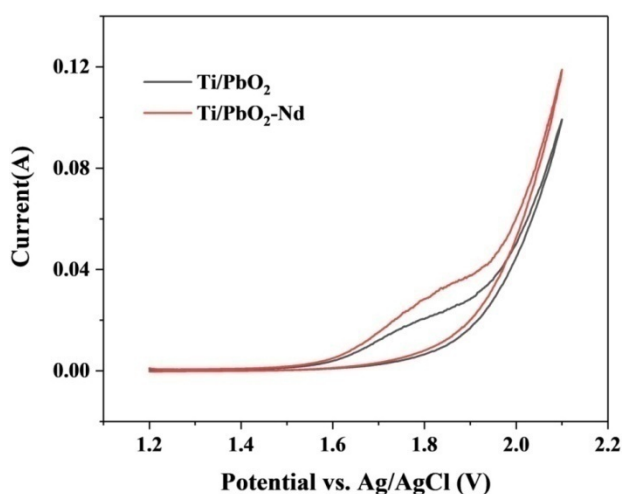


Figure 7. Curves of Ti/PbO₂ and Ti/PbO₂-Nd electrodes.

3.4. Energy Consumption

The energy consumptions of the Ti/PbO₂ and Ti/PbO₂-Nd electrode for electrocatalytic BPS oxidation were calculated. The energy consumption value of the Ti/PbO₂ electrode was 95.45 kWh m⁻³, 1.58 times higher than that of the Ti/PbO₂-Nd electrode (60.26 kWh m⁻³). The result indicates that BPS degradation on the Ti/PbO₂-Nd electrode can save 35.20 kWh m⁻³. Therefore, Nd-doping effectively reduces the energy consumption in the electrochemical removal of BPS.

3.5. Reusability Evaluation

To evaluate the stability of the Ti/PbO₂-Nd electrode, electrocatalytic oxidation of BPS was performed in three successive recycling experiments. Results show that the removal efficiency of BPS slightly decreased after three rounds of electrocatalytic oxidation (Figure 8), which may have been caused by a small partial corrosion and peeling of the active layer from the electrode surface. However, after three rounds of reaction, the degradation efficiency was still as high as 90.79%. Besides, no evident drop of the active layer was found during the degradation. Therefore, Ti/PbO₂-Nd electrode proved to be in good stability.

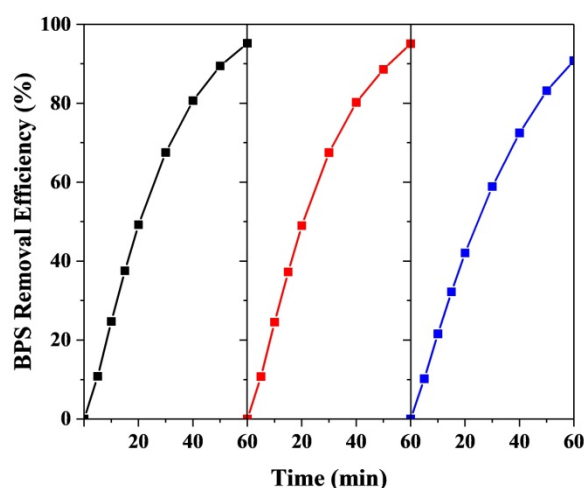


Figure 8. Reusability evaluation of bisphenol S degradation on Ti/PbO₂-Nd electrode (initial pH = 5.5; initial BPS concentration = 5 mg L⁻¹; T = 25 °C; Na₂SO₄ = 0.2 mol/L; current density = 15 mA cm⁻²).

3.6. Electrochemical Oxidation of BPS

3.6.1. Effect of Current Density on BPS Removal

It is well known that the current density determines the amount of hydroxyl radicals generated on the anode in the process of electro-oxidation. The influence of the current density on BPS removal is presented in Figure 9. As expected, the BPS removal efficiency rose with the increase of current density. After a 60-min degradation under different current densities from 5 to 25 mA cm⁻², the BPS removal efficiency surged from 35.76% to 98.47% significantly. Meanwhile, the value of k enhanced from 6.7 × 10⁻³ min⁻¹ to 64.8 × 10⁻³ min⁻¹. A reason for this can be that high current density facilitates the generation of hydroxyl radicals, which is conducive to the rapid degradation of pollutants. However, further analysis revealed that the k value has no distinct difference when the current density is up to 15 mA cm⁻². Therefore, 15 mA cm⁻² of current density was adopted for further study.

3.6.2. Effect of pH on BPS Removal

The influence of the initial pH value on BPS removal efficiency is presented in Figure 10. Results show that BPS removal efficiency decreased with the increase of pH value due to the increase of OEP caused by the acidic environment. The oxygen evolution side reaction was then prevented. Meanwhile,

more hydroxyl radicals were generated to enhance the removal efficiency of BPS. However, further analysis showed that the effect of pH on BPS removal by Ti/PbO₂-Nd electrode was not remarkable. With the increase of the pH, the removal efficiency of BPS decreased from 97% to 87%. Hence, the electrochemical oxidation of BPS by Ti/PbO₂-Nd can be used in a wide range of pH.

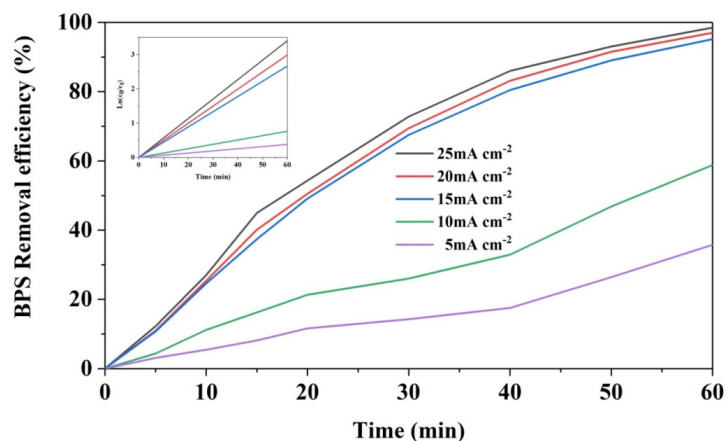


Figure 9. Effects of current density on BPS removal (initial pH = 5.5; initial BPS concentration: 5 mg L⁻¹; T = 25 °C; Na₂SO₄ = 0.2 mol/L).

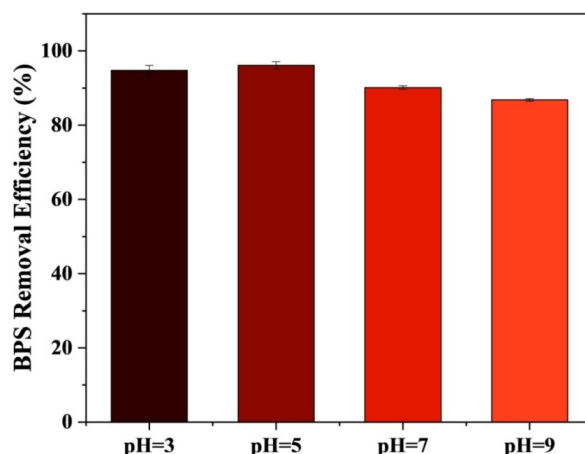


Figure 10. Effects of initial pH value on BPS removal efficiency (initial BPS concentration = 5 mg L⁻¹; T = 25 °C; Na₂SO₄ = 0.2 mol/L; current density = 15 mA cm⁻²).

3.7. Mechanism of the Electrochemical Oxidation of BPS by Ti/PbO₂-Nd

The PbO₂ anode is a "non-active electrode". Pollutants are destroyed mainly by indirect oxidation [35]. Cyclic voltammetry curves of the Ti/PbO₂-Nd electrode in the presence and absence of 5 mg L⁻¹ BPS were tested. The scan rate was set at 10 mV s⁻¹. The results are shown in Figure 11. No new peaks appeared when BPS was added, indicating that BPS is degraded via indirect ways on the Ti/PbO₂-Nd electrode by •OH radicals adsorbed on the electrode surface [21]. Results of scavenger experiments also show that •OH plays a key role in the electrochemical oxidation of BPS by Ti/PbO₂-Nd. Nd-doping contributes to finer crystalline grains and more surface areas. Thus, there are more •OH generated on the Ti/PbO₂-Nd electrode in order to improve the removal efficiency of BPS.

The interaction between the adsorbed hydroxyl radical and the electrode was weak. The weakly adsorbed hydroxyl radical was the physically adsorbed active oxygen (PbO₂(•OH)). The active oxygen with strong oxidizability could oxidize organics without selectivity, which means it could react with initial pollutants as well as intermediate products. The degradation of organics is also accompanied by the occurrence of an oxygen evolution reaction.

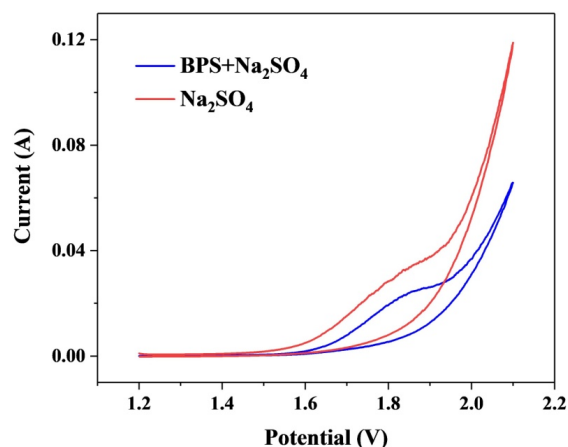


Figure 11. Cyclic voltammetry (CV) curves of the Ti/PbO₂-Nd electrode in the presence and absence of 5 mgL⁻¹ BPS.

To clearly investigate the main role of the active species involved in the electrocatalytic oxidation process, scavenger experiments were performed. Methanol was used as the •OH scavenger. As demonstrated in Figure 12, the removal efficiency of BPS decreased from 95.15% to 51.48% when methanol was added in the electrolyte on Ti/PbO₂-Nd. This may be explained because methanol can quickly consume the hydroxyl radicals generated in the system so that the amount of hydroxyl radicals involved in the degradation of BPS is reduced, namely, the degradation rate of BPS significantly decreases after the •OH is removed. Moreover, the removal efficiency decreased only from 85.20% to 47.06% on the Ti/PbO₂ electrode, indicating that the Ti/PbO₂-Nd can generate more •OH than that of Ti/PbO₂ electrode, which is consistent with the results of the LSV mentioned above.

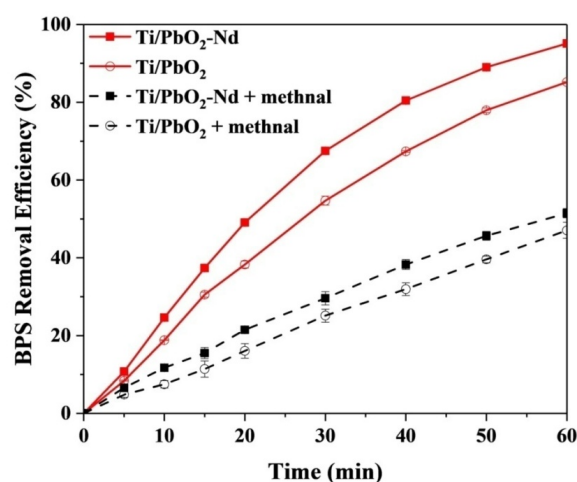


Figure 12. Effects of methanol on the BPS removal (initial pH = 5.5; initial BPS concentration = 5 mg L⁻¹; T = 25 °C; Na₂SO₄ = 0.2 mol/L; current density = 15 mA cm⁻²).

The HPLC-MS analysis was carried out to investigate the degradation pathways of BPS. Table 2 lists all intermediates that emerged during the intermediate analysis process. Based on the detected intermediates, a possible degradation pathway of BPS under electro-oxidation has been proposed, as shown in Figure 13.

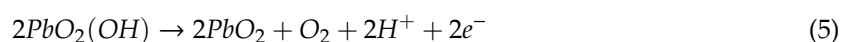
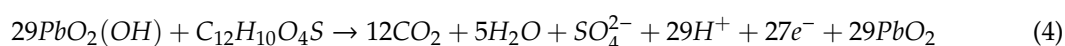
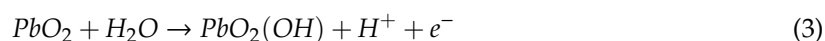


Table 2. The hypothetical chemical structures of the intermediates identified by HPLC-MS during the electrocatalytic degradation of BPS.

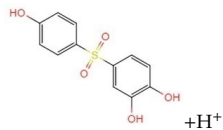
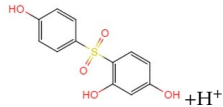
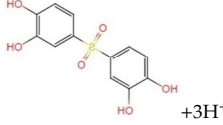
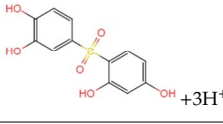
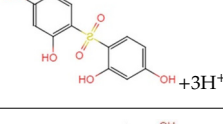
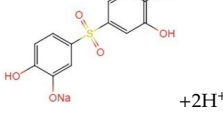
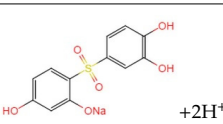
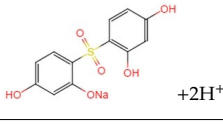
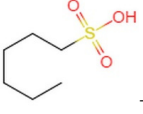
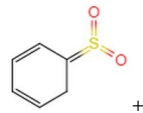
Retention Time (min)	Symbol	Mass (m/z)	Molecular Formula	Chemical Structure
7.533	a	267.1	$C_{12}H_{11}O_5S^+$	 +H ⁺
	b			 +H ⁺
2.071–3.053	c	285.0	$C_{12}H_{13}O_6S^{3+}$	 +3H ⁺
	d			 +3H ⁺
	e			 +3H ⁺
	f	306.9	$C_{12}H_{11}O_6SNa^{2+}$	 +2H ⁺
	g			 +2H ⁺
	h			 +2H ⁺
	i	165	$C_6H_{14}O_3S^-$	 -H ⁺
	j	143	$C_6H_7O_2S^+$	 +H ⁺

Figure 14 shows that BPS has two hydroxylation reactions before ring opening and oxidation. After that, part of the intermediate product hydrolyzes. The remaining matters are oxidized by radicals to more intermediate products and are finally mineralized into carbon dioxide. The aromatic products of $C_{12}H_{11}O_5S^+$ (a, b) are formed in the early degradation stage. As the electrolysis process proceeds, their concentrations drop. In other words, the main reaction in the early electro-oxidation stage is the hydroxylation of BPS. Then, a cleavage reaction of the aromatic intermediates follows due to the

increasing concentration of intermediate products i and j as mentioned in Table 2 and Figure 14. In the last period, cracking of the aromatic ring becomes the main reaction [36,37].

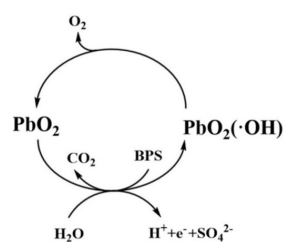


Figure 13. Oxidation process of the BPS on Ti/PbO₂-Nd electrode.

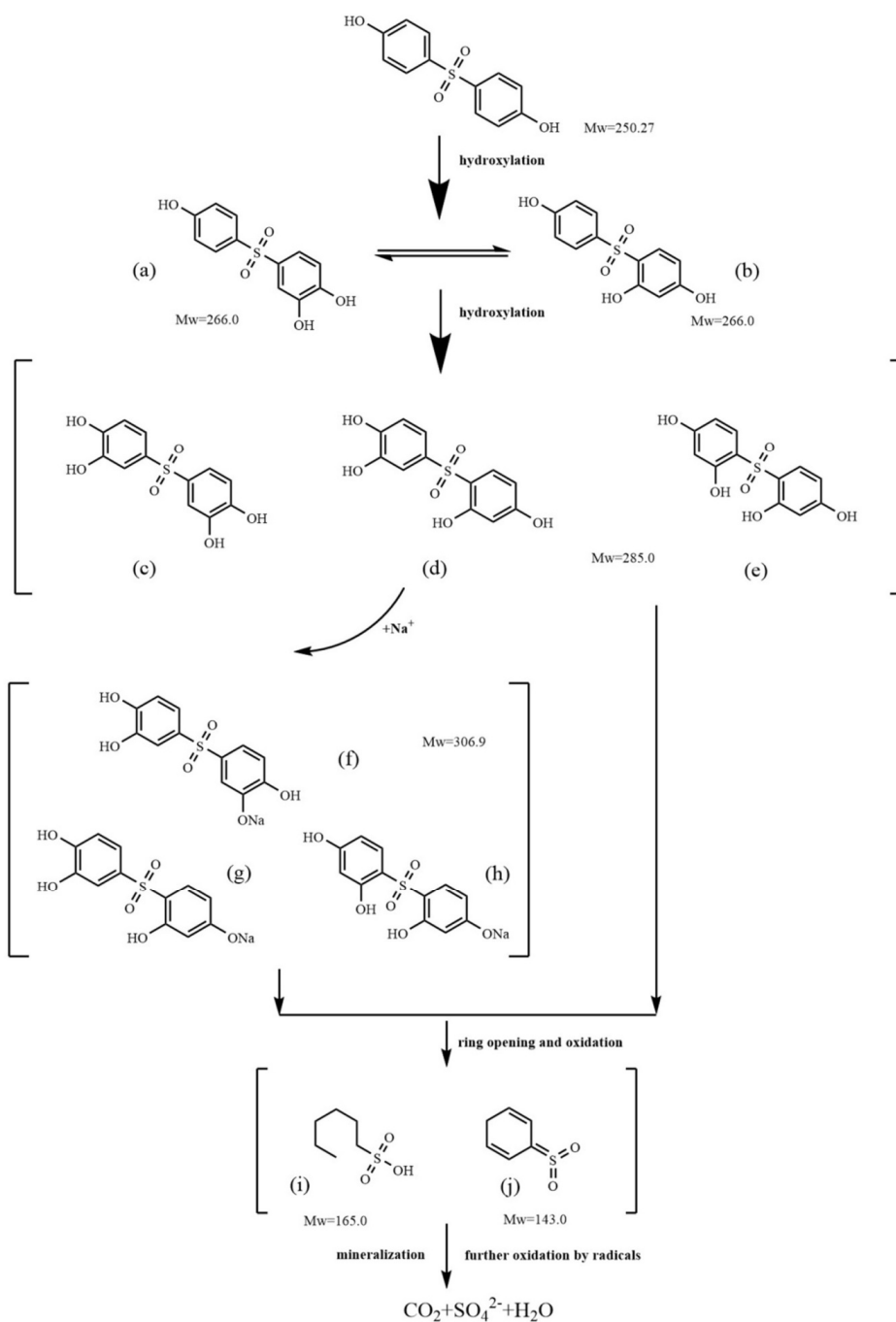


Figure 14. The hypothetical pathway of BPS degradation on the Ti/PbO₂-Nd electrode.

4. Conclusions

A series of Ti/PbO₂-Nd electrodes were fabricated by pulse electrodeposition. Nd-doping contributes to finer crystalline grains and more surface areas, which helps to generate more •OH to the oxidation of BPS. In addition, compared with the Ti/PbO₂ electrode, the surface of Ti/PbO₂-Nd electrodes has a finer grain size and a more compact structure. Besides, the decrease of pulse duty cycles from 100% to 50% also contributes to the tiny size of crystals. Compared to the traditional Ti/PbO₂ electrode, the OEP of the Ti/PbO₂-Nd electrodes increased from 1.41 V to 1.55 V (vs. Ag/AgCl). Meanwhile, •OH played a key role in the electrochemical oxidation of BPS by Ti/PbO₂-Nd, and BPS degradation obeyed the pseudo first-order kinetics model. A small amount of Nd doping contributes a lot in the degradation of BPS. Over 95% of BPS could be removed under a constant current density of 15 mA cm⁻². Additionally, the energy consumption of BPS degradation on the Ti/PbO₂-Nd electrode is 60.26 kWh m⁻³, which is much lower than that on the Ti/PbO₂ electrode. The HPLC-MS analysis confirms the intermediates, including the hydroxylation products and ring opening organics. The Ti/PbO₂-Nd electrode shows to be a promising anode material for electrocatalytic degradation of BPS.

Author Contributions: Conceptualization, Y.Z., Z.N.; investigation, Z.N., J.Y.; Data Curation, Z.N.; writing—original draft preparation, Z.N., Y.Z.; writing—review and editing, Y.Z., Z.N.; supervision, Y.Z.; funding acquisition, Y.Z. All authors have read and agreed to the published version of the manuscript.

Funding: This research received no external funding.

Acknowledgments: This research was supported by the National Science and Technology Major Project of China-Water Pollution Control and Treatment (2017ZX07201004).

Conflicts of Interest: The authors declare no conflict of interest. The sponsors had no role in the design, execution, interpretation, or writing of the study.

References

- Zhu, Q.Q.; Jia, J.B.; Wang, Y.; Zhang, K.G.; Zhang, H.; Liao, C.Y.; Jiang, G.B. Spatial distribution of parabens, triclocarban, triclosan, bisphenols, and tetrabromobisphenol A and its alternatives in municipal sewage sludges in China. *Sci. Total Environ.* **2019**, *679*, 61–69. [[CrossRef](#)]
- Shao, P.H.; Ren, Z.J.; Tian, J.Y.; Gao, S.S.; Luo, X.B.; Shi, W.X.; Yan, B.Y.; Li, J.; Cui, F.Y. Silica hydrogel-mediated dissolution-recrystallization strategy for synthesis of ultrathin A-Fe₂O₃ nanosheets with highly exposed (1 1 0) facets: A superior photocatalyst for degradation of bisphenol S. *Chem. Eng. J.* **2017**, *323*, 64–73. [[CrossRef](#)]
- Liao, C.Y.; Liu, F.; Moon, H.B.; Yamashita, N.; Yun, S.H.; Kannan, K. Bisphenol analogues in sediments from industrialized areas in the United States, Japan, and Korea: Spatial and temporal distributions. *Environ. Sci. Technol.* **2012**, *46*, 11558–11565. [[CrossRef](#)] [[PubMed](#)]
- Jin, H.B.; Zhu, L.Y. Occurrence and partitioning of bisphenol analogues in water and sediment from Liaohe River Basin and Taihu Lake, China. *Water Res.* **2016**, *103*, 343–351. [[CrossRef](#)] [[PubMed](#)]
- Mathew, M.; Sreedhanya, S.; Manoj, P.; Aravindakumar, C.T.; Aravind, U.K. Exploring the interaction of bisphenol-S with serum albumins: A better or worse alternative for bisphenol A? *J. Phys. Chem. B* **2014**, *118*, 3832–3843. [[CrossRef](#)] [[PubMed](#)]
- Liao, C.Y.; Liu, F.; Alomirah, H.; Loi, V.D.; Mohd, M.A.; Moon, H.B.; Nakata, H.; Kannan, K. Bisphenol S in urine from the United States and seven Asian countries: Occurrence and human exposures. *Environ. Sci. Technol.* **2012**, *46*, 6860–6866. [[CrossRef](#)]
- Eladak, S.; Grisin, T.; Moison, D.; Guerin, M.J.; N'Tumba-Byn, T.; Pozzi-Gaudin, S.; Benachi, A.; Livera, G.; Rouiller-Fabre, V.; Habert, R. A new chapter in the bisphenol a story: Bisphenol S and bisphenol F are not safe alternatives to this compound. *Fertil. Steril.* **2015**, *103*, 11–21. [[CrossRef](#)]
- Wang, Y.Q.; Zhang, H.M. Effects of bisphenol s on the structures and activities of trypsin and pepsin. *J. Agric. Food Chem.* **2014**, *62*, 11303–11311. [[CrossRef](#)]
- Liu, Y.; Guo, H.G.; Zhang, Y.L.; Cheng, X.; Zhou, P.; Wang, J.Q.; Li, W. Fe@C carbonized resin for peroxydisulfate activation and bisphenol S degradation. *Environ. Pollut.* **2019**, *252*, 1042–1050. [[CrossRef](#)]

10. Zhang, T. Research Progress on Peroxymonosulfate Activation Technology. *Guangdong Chem. Ind.* **2019**, *46*, 122–123.
11. López-Ramón, M.V.; Ocampo-Pérez, R.; Bautista-Toledo, M.I.; Rivera-Utrilla, J.; Moreno-Castilla, C.; Sánchez-Polo, M. Removal of bisphenols A and S by adsorption on activated carbon clothes enhanced by the presence of bacteria. *Sci. Total Environ.* **2019**, *669*, 767–776. [[CrossRef](#)] [[PubMed](#)]
12. Chen, Y.; Li, H.Y.; Liu, W.J.; Tu, Y.; Zhang, Y.H.; Han, W.Q.; Wang, L.J. Electrochemical degradation of nitrobenzene by anodic oxidation on the constructed TiO₂-NTs/SnO₂-Sb/PbO₂ electrode. *Chemosphere.* **2014**, *113*, 48–55. [[CrossRef](#)] [[PubMed](#)]
13. Zhang, X.N.; Huang, W.M.; Wang, X.; Gao, Y.; Lin, H.B. Feasibility and advantage of biofilm-electrode reactor for phenol degradation. *J. Environ. Sci.* **2009**, *21*, 1181–1185. [[CrossRef](#)]
14. Chen, J.M.; Xia, Y.J.; Dai, Q.Z. Electrochemical degradation of chloramphenicol with a novel Al doped PbO₂ electrode: Performance, kinetics and degradation mechanism. *Electrochim. Acta* **2015**, *165*, 277–287. [[CrossRef](#)]
15. Xu, H.; Zhang, Q.; Yan, W.; Chu, W.; Zhang, L.F. Preparation and characterization of PbO₂ electrodes doped with TiO₂ and its degradation effect on azo dye wastewater. *Int. J. Electrochem. Sci.* **2013**, *8*, 5382–5395.
16. Li, X.L.; Li, X.M.; Yang, W.J.; Chen, X.H.; Li, W.L.; Luo, B.B.; Wang, K.L. Preparation of 3D PbO₂ nanospheres@SnO₂ nanowires/Ti Electrode and Its Application in Methyl Orange Degradation. *Electrochim. Acta* **2014**, *146*, 15–22. [[CrossRef](#)]
17. Kotyk, J.F.K.; Chen, C.; Sheehan, S.W. Corrosion Potential Modulation on Lead Anodes Using Water Oxidation Catalyst Coatings. *Coatings.* **2018**, *8*, 246. [[CrossRef](#)]
18. Li, S.P.; Wang, H.B.; Qiao, P.; Zhou, X.Y. Study on the treatment of printing and dyeing wastewater with the new type of Ni—Doped PbO₂/Ti electrode. *Ind. Water Treat.* **2008**, *28*, 48–51.
19. Xu, H.; Li, J.J.; Yan, W.; Chu, W. Preparation and characterization of titanium based PbO₂ electrodes doped with some common elements. *Rare Met. Mater. Eng.* **2013**, *42*, 885–890.
20. Dai, Q.Z.; Zhou, J.Z.; Weng, M.L.; Luo, X.B.; Feng, D.L.; Chen, J.M. Electrochemical oxidation metronidazole with Co modified PbO₂ electrode: Degradation and mechanism. *Sep. Purif. Technol.* **2016**, *166*, 109–116. [[CrossRef](#)]
21. Dai, Q.Z.; Xia, Y.J.; Chen, J.M. Mechanism of enhanced electrochemical degradation of highly concentrated aspirin wastewater using a rare earth La-Y co-doped PbO₂ electrode. *Electrochim. Acta* **2016**, *188*, 871–881. [[CrossRef](#)]
22. Xu, M.; Wang, Z.C.; Wang, F.W.; Hong, P.; Wang, C.Y.; Ouyang, X.M.; Zhu, C.G.; Wei, Y.J.; Hun, Y.H.; Fang, W.Y. Fabrication of cerium doped Ti/nanoTiO₂/PbO₂ electrode with improved electrocatalytic activity and its application in organic degradation. *Electrochim. Acta* **2016**, *201*, 240–250. [[CrossRef](#)]
23. Feng, Y.J.; Ding, H.; Zhang, W.J. Research on electrocatalytic properties of rare earth doped Ti/SnO₂-Sb electrodes by CV and Tafel curves. *Mater. Sci. Technol.* **2009**, *17*, 278–280+284.
24. Sun, Z.R.; Zhang, H.; Wei, X.F.; Du, R.; Hu, X. Fabrication and electrochemical properties of a SnO₂-Sb anode doped with Ni-Nd for phenol oxidation. *J. Electrochem. Soc.* **2015**, *162*, H590–H596. [[CrossRef](#)]
25. Yao, Y.W.; Zhao, C.M.; Zhao, M.M.; Wang, X. Electrocatalytic degradation of methylene blue on PbO₂-ZrO₂ nanocomposite electrodes prepared by pulse electrodeposition. *J. Hazard. Mater.* **2013**, *263*, 726–734. [[CrossRef](#)] [[PubMed](#)]
26. Yao, Y.W.; Zhao, M.M.; Zhao, C.M.; Wang, X. Preparation and Characterization of PbO₂ Electrodes Prepared by Pulse Electrodeposition with Different Pulse Frequency. *J. Electrochem. Soc.* **2013**, *160*, D553–D557. [[CrossRef](#)]
27. Duan, X.Y.; Ma, F.; Yuan, Z.X.; Chang, L.M.; Jin, X.T. Comparative studies on the electro-catalytic oxidation performance of surfactant-carbon nanotube-modified PbO₂ electrodes. *J. Electroanal. Chem.* **2012**, *677*, 90–100. [[CrossRef](#)]
28. Feng, J.R.; Johnson, D.C. Electrocatalysis of anodic oxygen-transfer reactions: Titanium substrates for pure and doped lead dioxide films. *J. Electrochem. Soc.* **1991**, *138*, 3328–3337. [[CrossRef](#)]
29. He, Z.Q.; Zhou, J.J.; Huang, X.W.; Zhang, S.H.; Song, S. Enhancement of the Activity and Stability of PbO₂ Electrodes by Modifying with Polydimethylsiloxane. *J. Electrochem. Soc.* **2018**, *165*, H717–H724. [[CrossRef](#)]
30. Qiao, Q.C.; Singh, S.; Lo, S.L.; Li, Y.; Jin, J.R.; Wang, L.Z. Electrochemical oxidation of acid orange 7 dye with Ce, Nd, and Co-modified PbO₂ electrodes: Preparation, characterization, optimization, and mineralization. *J. Taiwan Inst. Chem. Eng.* **2018**, *84*, 110–122. [[CrossRef](#)]

31. Darabizad, G.; Rahmanifar, M.S.; Mousavi, M.F.; Pendashteh, A. Electrodeposition of morphology- and size-tuned PbO₂ nanostructures in the presence of PVP and their electrochemical studies. *Mater. Chem. Phys.* **2015**, *156*, 121–128. [[CrossRef](#)]
32. Zhao, B.; Yu, H.B.; Lu, Y.; Qu, J.; Zhu, S.Y.; Huo, M.X. Polyethylene glycol assisted synthesis of a praseodymium-doped PbO₂ electrode and its enhanced electrocatalytic oxidation performance. *J. Taiwan Inst. Chem. Eng.* **2019**, *100*, 144–150. [[CrossRef](#)]
33. Wu, T.; Zhao, G.H.; Lei, Y.Z.; Li, P.Q. Distinctive tin dioxide anode fabricated by pulse electrodeposition: High oxygen evolution potential and efficient electrochemical degradation of fluorobenzene. *J. Phys. Chem. C.* **2011**, *115*, 3888–3898. [[CrossRef](#)]
34. Comninellis, C. Electrocatalysis in the electrochemical conversion/combustion of organic pollutants for waste water treatment. *Electrochim. Acta* **1994**, *39*, 1857–1862. [[CrossRef](#)]
35. Shih, Y.J.; Huang, Y.H.; Huang, C.P. Oxidation of ammonia in dilute aqueous solutions over graphite-supported α - and β -lead dioxide electrodes (PbO₂@G). *Electrochim. Acta* **2017**, *257*, 444–454. [[CrossRef](#)]
36. Yang, X.P.; Zou, R.Y.; Huo, F.; Cai, D.C.; Xiao, D. Preparation and characterization of Ti/SnO₂-Sb₂O₃-Nb₂O₅/PbO₂ thin film as electrode material for the degradation of phenol. *J. Hazard. Mater.* **2009**, *164*, 367–373. [[CrossRef](#)]
37. He, Z.; Hayat, M.D.; Huang, S.F.; Wang, X.G.; Cao, P. PbO₂ electrodes prepared by pulse reverse electrodeposition and their application in benzoic acid degradation. *J. Electroanal. Chem.* **2018**, *812*, 74–81. [[CrossRef](#)]



© 2020 by the authors. Licensee MDPI, Basel, Switzerland. This article is an open access article distributed under the terms and conditions of the Creative Commons Attribution (CC BY) license (<http://creativecommons.org/licenses/by/4.0/>).